ChemPubSoc Europe

https://doi.org/10.1002/ejic.201800297

EurJIC European Journal of Inorganic Chemistry

Full Paper

Check for updates

Organometallic Chemistry

N,N′-Diamidonaphthalene as a Versatile Ligand to Stabilize Mono- and Bimetallic Complexes of Group 13

Sojung Lee,[a] Nawal Almalki,[a] Bulat Gabidullin,[a] and Darrin Richeson*[a]

Abstract: Disubstituted 1,8-diamidonaphthalene complexes of B and Al were accessed via hydrogen or methane elimination reactions from readily available borane or trimethylaluminum. Trigonal planar borane complexes, HB[1,8-(NR)$C_{10}H_6$] (R = *i*Pr, **4** and R = Ph, **5**), were observed to be air stable, a feature attributed to B–N pπ–pπ bonding and supported by computations. Bimetallic Al complexes, $[Al(CH_3)_2]_2[(RN)_2C_{10}H_6]$ (R = *i*Pr, **7**, R = Ph, **8**, or R = *i*Pr/Np, **9**), were documented by single-crystal X-ray diffraction analyses and display puckered, four-membered M_2N_2 rings with a bridging diamidonaphthalene ligand. With R = Ph, a monometallic aluminum complex, $MeAl(OEt_2)$-[1,8-$(PhN)_2C_{10}H_6$] (**6**), was isolated as a diethylether adduct. The structural data suggested that the dialkyl and diaryl are stronger σ-bonding ligands compared to reported trimethylsilyl analogues.

Introduction

Boron hydrides and alkylaluminum species are core functional groups in the chemistry of the group 13 elements. They can be exploited from both fundamental and applied perspectives and have been employed for their reactivity and as building blocks in synthesis. Modulation of the chemistry of these and other group 13 element functionalities can be achieved through changes to the ligand environment. For example, the application of β-diketiminate ligands has vitalized the synthetic chemistry of group 13 elements.[1–4] As supporting ligands, β-diketiminates exhibit strong and diverse binding modes combined with adjustable steric demands through variation of the NR substituents and these features have promoted their application in group 13 and across the periodic Table These observations provided an impetus for our efforts to design and implement ligands that are reminiscent of the β-diketiminate scaffold in both geometry and frontier orbital topology and this target has led us to investigate the application of the dianions, *N,N′*-disubstituted-1,8-diamidonaphthalene ("R_2DAN^{2-}") as ligands in group 13 chemistry. The R_2DAN^{2-} scaffold presents a rigid dianionic ligand with delocalized π-electrons in a framework with similarities to the β-diketiminate scaffold. Diaminonaphthalene-based ligands have seen some application with borohydride and alkylaluminum chemistry with particularly noteworthy examples being silyl-substituted tetraminoperylene and 1,8-bis(trialkylsilylamino)naphthalene group 13 compounds represented by **A**–**D**.[5–9] Importantly, reports have been restricted to trialkylsilyl, R_3Si, substituents and are therefore limited by the electronic, steric and potential *N*-silyl reactivity of these groups.

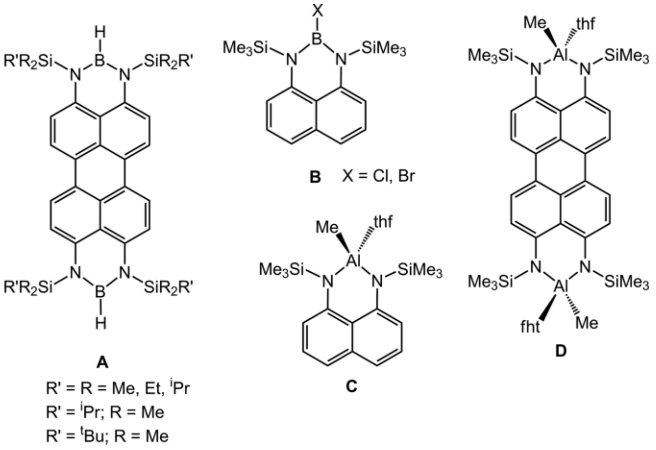

Our desire is to explore the modification to the steric and electronic features of the R_2DAN^{2-} framework by introduction and variation of the N-substituents to include both alkyl and aryl groups. We previously reported the syntheses of ligands **1**–**3** (Scheme 1) through a multi-step reductive amination method,[10] or using a Cu catalyzed coupling reaction,[11–13] respectively. Furthermore, among the main group elements, this framework has been successfully applied to group 14 divalent species[10,14,15] and to low coordinate group 15 cations.[16,17] We now wish to report the use three disubstituted 1,8-diaminonaphthalene species **1**–**3**[15] for the isolation and characterization of monomeric, three coordinate borohydrides with unusual air stability as well as mono- and dinuclear Al-Me complexes. These new compounds make a substantial and fundamental contribution to the limited number of compounds reported with the 1,8-diamidonaphthalene-based scaffold and represent potential building blocks for further synthetic chemistry of these elements.

---

[a] Department of Chemistry and Biomolecular Sciences and Centre for Catalysis Research and Innovation, University of Ottawa,
Ottawa, Ontario K1N6N5, Canada
E-mail: darrin@uottawa.ca
http://mysite.science.uottawa.ca/darrin/

Supporting information and ORCID(s) from the author(s) for this article are available on the WWW under https://doi.org/10.1002/ejic.201800297.

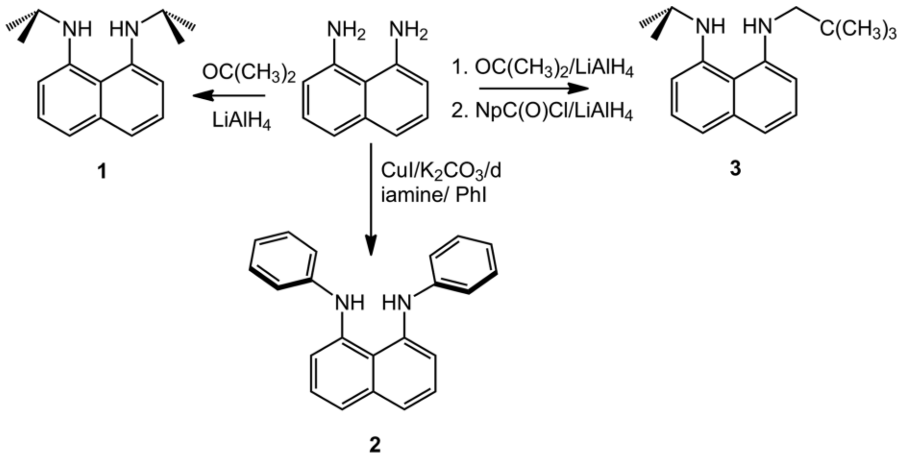

Scheme 1. Synthetic routes to ligands **1**, **2** and **3**.

Results and Discussion

The diaminonaphthalene proligands **1**–**3** possess reactive NH protons allowing for their direct reaction with inorganic and organometallic compounds that possess basic groups. These compounds include boron hydrides, with reactive BH groups, and trimethylaluminum with strongly basic AlMe moieties. For example, both **1** and **2** react directly with $BH_3(SMe_2)$ as summarized in Scheme 2. From these reactions, compounds **4** and **5** were isolated as colorless and light orange crystals, respectively. The multi-nuclear NMR spectra of these two new 1,3,2-diazaborine species provide clear indications for the structures proposed for **4** and **5**. Specifically, both compounds exhibited ^1H and ^{13}C NMR resonances indicating a symmetrical ligation for the R_2DAN^{2-} group. A broad resonance for the BH group was observed in each of the ^1H NMR spectra at δ = 4.74 ppm (**4**) and 4.26 ppm (**5**) with these values being comparable to silylated *N,N′;N′′,N′′′*-diborylene-3,4,9,10-tetraaminoperylenes (**A**), which gave corresponding B-H resonances observed at δ = 4.71–4.75 ppm.[8] The ^{11}B NMR spectra further support the proposed formulations with compound **4** displaying a proton decoupled ^{11}B resonance at δ = 28.4 ppm while compound **5** showed such a resonance at δ = 25.9 ppm. For comparison, the perylene analogue **A** (R = Me) had a ^{11}B resonance at δ = 29.8 ppm.[7] Although they are not completely analogous, the monomeric species **B**, $BX[(NSiMe_3)_2C_{10}H_6]$, gave ^{11}B NMR resonances at similar chemical shifts of 32.1 ppm (X = Cl) and 28.0 ppm (X = Br).[6] Finally, the microanalysis data on **4** and **5** was consistent with the suggested formulations.

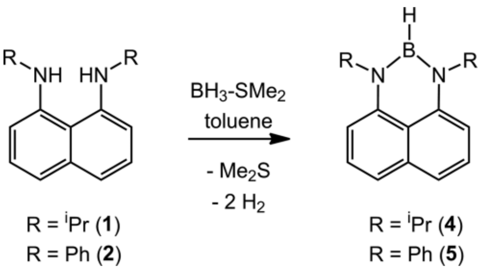

Scheme 2. Synthesis of compounds **4** and **5**.

Interestingly, both **4** and **5** are stable to air in both solid state and in solution and NMR solutions of these compounds can be prepared in the air using deuterated solvents directly from the bottle as received from the supplier. These observations are in sharp contrast with the reactivity of the diazaborine species **A**, which are sensitive in both solid state and solution.[8] Similarly, five-membered 2-hydrido-1,3,2-diazaboroles are reported to be colorless air- and moisture-sensitive solids.[18]

Definitive confirmation for the structural features of **4** and **5** was obtained from the single-crystal X-ray analyses and results are summarized in Figure 1 and Figure 2 and selected bond lengths and angles are given in Table 1. Both structures display a diamidonaphthalene group chelating to a trigonal planar B center. The NBN unit and naphthalene backbone are nearly coplanar with the angle between these two planes being only 4.5^0 in **4** and 8.2^0 in **5**. For both **4** and **5**, the H atom bonded to B were refined freely and yielded average B–H bond lengths of 1.11 Å. Both compounds exhibited similar N–B–N bite angles of $120.8(3)^0$ in **4** and $119.2(1)^0$in **5**, a feature that is consistent with sp^2 hybridized B centers. Finally, the B centers are bonded symmetrically to the ligand with **4** displaying two equal B–N distances [1.405(5) and 1.409(5) Å] and **5** showing slightly longer but equivalent distances at 1.4163(16) Å and

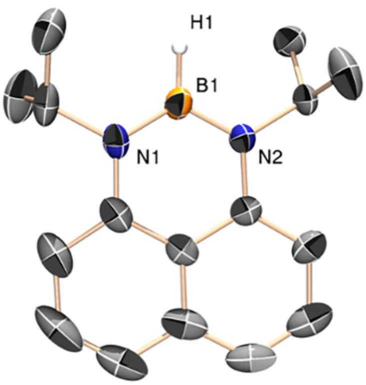

Figure 1. Structural representation of $HB[1,8-(iPrN)_2C_{10}H_6]$ (**4**). Carbon-bound hydrogen atoms have been omitted for clarity. The thermal ellipsoids are shown at 50 % probability level.

1.4186(16) Å. These bond lengths are, in both cases, slightly shorter than those reported for the tetraaminoperylene compounds **A**, which averaged 1.43 Å[8] Reported six-membered compounds with saturated rings, $HB(RR'C_6H_3NCHMe)_2CMe_2$ (R = R′ = *i*Pr; R = *i*Pr, R′ = H), displayed B–N distances that ranged from 1.396(4) Å to 1.414(5) Å and these distances were judged to optimize B–N pπ–pπ interactions.[19]

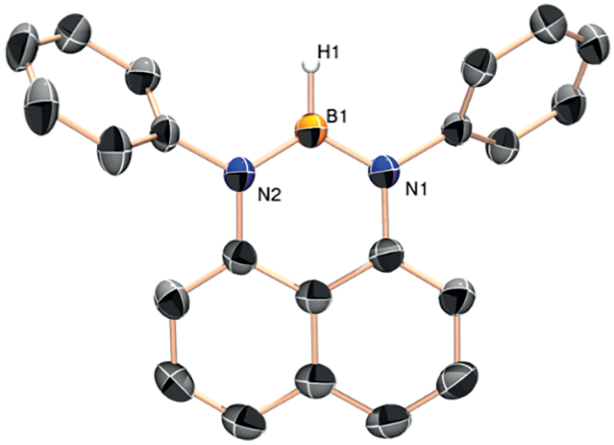

Figure 2. Structural representation of $HB[1,8\text{-}(PhN)_2C_{10}H_6]$ (**5**). Carbon-bound hydrogen atoms have been omitted for clarity. The thermal ellipsoids are shown at 50 % probability level.

Table 1. Selected bond lengths [Å] and angles [°] for $HB[(i\text{PrN})_2C_{10}H_6]$ (**4**) and $HB[(PhN)_2C_{10}H_6]$ (**5**).

Compound **4**		Compound **5**	
N(1)–B(1)	1.405(5)	B(1)–N(1)	1.4163(16)
N(2)–B(1)	1.409(5)	B(1)–N(2)	1.4186(16)
B(1)–H(1)	1.11(4)	B(1)–H(1)	1.112(13)
N(1)–B(1)–N(2)	120.8(3)	N(1)–B(1)–N(2)	119.21(11)
N(1)–B(1)–H(1)	123(2)	N(1)–B(1)–H(1)	119.5(7)
N(2)–B(1)–H(1)	115(2)	N(2)–B(1)–H(1)	121.3(7)
C(1)–N(1)–B(1)	120.6(3)	C(2)–N(1)–B(1)	120.84(10)
C(1)–N(1)–C(11)	118.5(3)	C(2)–N(1)–C(11)	118.89(9)
B(1)–N(1)–C(11)	120.6(3)	B(1)–N(1)–C(11)	120.27(10)
C(9)–N(2)–B(1)	120.2(3)	C(10)–N(2)–B(1)	121.07(10)
C(9)–N(2)–C(14)	119.2(7)	C(10)–N(2)–C(17)	119.49(9)
B(1)–N(2)–C(14)	120.7(7)	B(1)–N(2)–C(17)	119.41(10)

The air stability of **4** and **5** as well as the observed B–N bond lengths could be attributed to B–N π-bonding and in order to further reveal the more detailed features of these interactions we carried out a computational study on compound **4**. Starting with the crystal structure data, compound **4** was optimized using DFT and the Gaussian 09 program employing the B3LYP functional and a 6-311+G(d,p) basis set.[20] The resulting structure was well aligned with the experimentally determined X-ray data with comparison details provided in the Supporting Information.

The frontier orbitals obtained from these computations show a clear NBN π bonding interaction as presented in Figure 3. While the HOMO and LUMO for **4** are non-bonding with respect the BN linkages, the occupied HOMO-2 and HOMO-1 orbitals show the contribution to NBN π-bonding. Taken together the experimental as well as the theoretical data agree with a significant delocalization of the nitrogen 2*p*-centered lone electron pairs into the vacant $2p_z$ orbital of the boron atom in **4**.

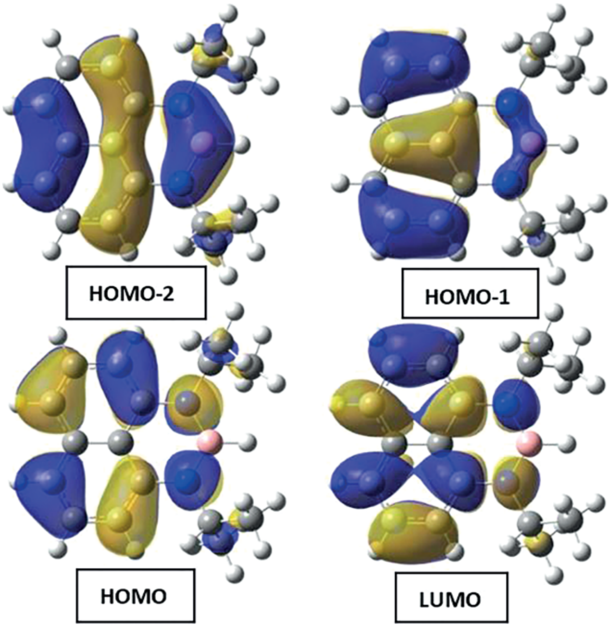

Figure 3. The frontier orbitals (HOMO-2 to LUMO) representing the π-bonding in **3** obtained from DFT [B3LYP, 6-311+G(d,p)] on compound **4**.

The protonation reaction of trimethylaluminum with ligand **2** in ether offers an analogous method for introducing the 1,8-$(PhN)_2C_{10}H_6^{2-}$ group in aluminum chemistry as shown in Scheme 3. The red crystalline product obtained from this reaction gave ^1H NMR spectroscopic data indicative of a 1:1 CH_3Al/ligand ratio and only nine aromatic carbon resonances in the ^{13}C NMR consistent with a symmetrical ligand environment. A ^1H resonance at $\delta = 0.24$ ppm was assigned the Al–CH_3 moiety and is comparable to the only analogues in the literature, compounds **C** and **D**, which displayed corresponding resonances, assigned to Al–CH_3, at $\delta = -0.55$ ppm and -0.57 ppm, respectively.[5,7]

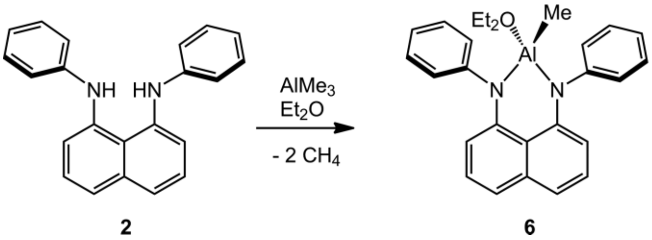

Scheme 3. Synthesis of compound **6**.

The NMR spectra of **6** showed variable traces of Et_2O and this provided further motivation to perform the single-crystal X-ray analysis on this species. The results of this analysis are summarized in Figure 4 with selected bond lengths and angles in Table 2. Compound **6** was the anticipated mononuclear Al species possessing one chelating *N,N′*-diphenyldiamidonaphthalene ligand, one methyl group and a coordinated diethyl ether to give a pseudo-tetrahedral coordination geometry for the Al center. The presence of coordinated ether is consistent with the fact that the crystals of **6** were removed from the mother liquor and immediately frozen in Paratone oil in preparation for the data collection. The N(1) and N(2) centers are planar with a sum of bond angles equal to 360^0 in both cases. Of the six angles around the Al center, the smallest is represented by the ligand bite angle N(1)–Al(1)–N(2), $98.84(11)^0$ and the average of these six angles is 109.3^0 supporting a distorted tetrahedral assignment. The four bond lengths associated with the Al center, C(23)–Al(1) = 1.939(3) Å, N(1)–Al(1) = 1.812(2) Å, N(2)–Al(1) = 1.816(2) Å, and Al(1)–O(1) = 1.895(2) Å, are slightly shorter than in the analogue $[1,8\text{-}(Me_3SiN)_2C_{10}H_6]$-Al(Me)thf (**C**) [Al–C 1.9482(16), av. Al–N = 1.830 Å, Al–O = 1.920 Å].[5] Further comparison can be made to the silylated tetraaminoperylenes species, $[AlMe(thf)]_2[(Me_3Si)_4N_4C_{20}H_8]$ (**D**), with Al–C = 1.954(3) Å, average Al–N = 1.826 Å, and Al–O = 1.910(2) Å.[7]

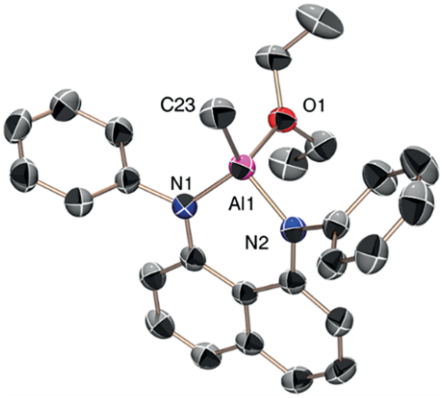

Figure 4. The molecular structure for $MeAl(OEt_2)[1,8\text{-}(PhN)_2C_{10}H_6]$ (**6**). Hydrogen atoms have been omitted for clarity. The thermal ellipsoids are shown at 50 % probability level.

Table 2. Selected bond lengths [Å] and angles [°] for $Al(CH_3)(Et_2O)$-$[(PhN)_2C_{10}H_6]$ (**6**).

C(23)–Al(1)	1.939(3)	N(2)–Al(1)	1.816(2)
N(1)–Al(1)	1.812(2)	Al(1)–O(1)	1.895(2)
C(1)–N(1)–Al(1)	125.0(2)	N(1)–Al(1)–O(1)	108.21(10)
C(11)–N(1)–Al(1)	118.01(18)	N(2)–Al(1)–O(1)	103.83(10)
C(9)–N(2)–C(17)	118.9(2)	N(1)–Al(1)–C(23)	117.73(13)
C(9)–N(2)–Al(1)	124.79(19)	N(2)–Al(1)–C(23)	119.84(13)
C(17)–N(2)–Al(1)	116.20(18)	O(1)–Al(1)–C(23)	107.17(12)
N(1)–Al(1)–N(2)	98.84(11)		

The longer bond lengths for the *N*-silyl species parallels the observations with the boron compounds **4** and **5** and these features imply that ligands **1** and **2** may have slightly stronger element–ligand bonding interactions.

The reaction of $AlMe_3$ with ligand **1** followed a different path than for the synthesis of **6**. The direct reaction of equimolar ratio of **1** and $AlMe_3$ proceeded smoothly to yield the unanticipated bimetallic product $(AlMe_2)_2[1,8\text{-}(i\text{PrN})_2C_{10}H_6]$ (**7**) as shown in Scheme 4. The first indication of a bimetallic species was the appearance of two equal intensity (6 H) proton NMR signals at δ = –0.10 ppm and –1.18 ppm consistent with four Al–CH_3 groups. Furthermore, the ^1H NMR spectrum of **7** displayed two equal integral doublet peaks at δ = 1.38 ppm and 1.28 ppm assigned to the methyl groups of the *i*Pr substituents.

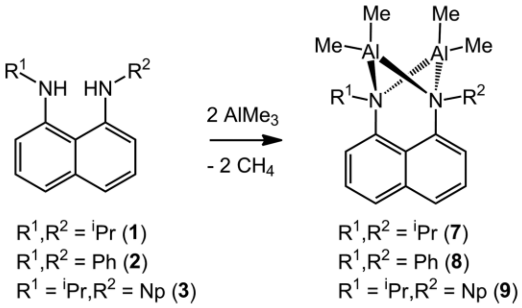

Scheme 4. Synthesis of compounds **7**–**9**.

Surprisingly, this product was the only isolated species regardless of the reaction stoichiometry between **1** and $AlMe_3$ and an improved synthesis was achieved using 2 equiv. of $AlMe_3$ to produce **7** which could be obtained as colorless crystals from cold (–25 °C) ether. An X-ray diffraction study was performed and confirmation of the connectivity was obtained with the molecular structure shown in Figure 5. The corresponding values for selected bond lengths and angles are provided in Table 3.

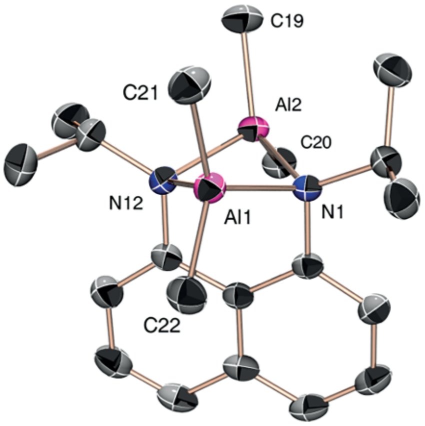

Figure 5. The molecular structure for $(AlMe_2)_2[1,8\text{-}(i\text{PrN})_2C_{10}H_6]$ (**7**). Hydrogen atoms have been omitted for clarity. The thermal ellipsoids are shown at 50 % probability level.

Compound **7** is a bimetallic Al species, $[\mu\text{-}1,8\text{-}(i\text{PrN})_2\text{-}C_{10}H_6](AlMe_2)_2$, with each aluminum center possessing a four-coordinate distorted tetrahedral geometry consisting of two methyl groups, and the two nitrogens of a 1,8-diamidonaphthalene ligand. Each of the anionic nitrogen centers formally possesses two electron pairs and both of these are donated to the two different Al centers. The result is a puckered, butterfly shaped Al_2N_2 metallacycle with approximate C_{2v} symmetry. A similar structure has been reported from the related trimethylsilyl ligand, $[\mu\text{-}1,8\text{-}(Me_3SiN)_2C_{10}H_6](AlMe_2)_2$ (**E**).[9] The four Al–N bond lengths in **7** range from 1.9710(15) Å to 1.9873(15) Å and are considerably longer than in the mononuclear species **6** yet slightly shorter than in compound **E** with Al–N of 1.998(4) and 1.995(4) Å. The bimetallic core positions the two methyls on each Al in inequivalent environments consistent with the NMR

Table 3. Selected bond lengths [Å] and angles [°] for $[Al(CH_3)_2]_2[(iPrN)_2C_{10}H_6]$ (**7**).

Al(1)–C(21)	1.962(2)	Al(2)–C(19)	1.9554(19)
Al(1)–C(22)	1.9627(19)	Al(2)–C(20)	1.957(2)
Al(1)–N(12)	1.9744(17)	Al(2)–N(12)	1.9710(15)
Al(1)–N(1)	1.9836(15)	Al(2)–N(1)	1.9873(15)
C(21)–Al(1)–C(22)	116.15(10)	C(2)–N(1)–C(13)	114.34(14)
C(21)–Al(1)–N(12)	112.00(8)	C(2)–N(1)–Al(1)	103.76(10)
C(22)–Al(1)–N(12)	113.17(8)	C(13)–N(1)–Al(1)	117.48(12)
C(21)–Al(1)–N(1)	115.90(8)	C(2)–N(1)–Al(2)	103.09(11)
C(22)–Al(1)–N(1)	113.85(8)	C(13)–N(1)–Al(2)	122.91(11)
N(12)–Al(1)–N(1)	80.74(6)	Al(1)–N(1)–Al(2)	91.59(6)
C(21)–Al(1)–Al(2)	102.91(7)	C(10)–N(12)–C(16)	119.72(15)
C(19)–Al(2)–C(20)	114.93(9)	C(10)–N(12)–Al(2)	106.45(11)
C(19)–Al(2)–N(12)	109.74(8)	C(16)–N(12)–Al(2)	114.31(11)
C(20)–Al(2)–N(12)	114.90(8)	C(10)–N(12)–Al(1)	104.45(11)
C(19)–Al(2)–N(1)	119.14(8)	C(16)–N(12)–Al(1)	115.74(12)
C(20)–Al(2)–N(1)	112.81(8)	Al(2)–N(12)–Al(1)	92.35(7)
N(12)–Al(2)–N(1)	80.73(6)		

observations. Crystallographically there are four Al–C bond lengths ranging from 1.9554(19) Å to 1.9627(19) Å. In **7** the two N–Al–N bite angles were $80.74(6)^0$ and $80.73(6)^0$ which are much smaller than the corresponding angle in **6** but only slightly smaller than the angle of 83.0(2)° observed for compound **E**.

Employing this same stoichiometric ratio but using ligand **2** or **3** generated the analogous bimetallic Al species **8** and **9** (Scheme 4). The appearance of two inequivalent, equal intensity signals assigned to the Al–CH_3 groups in the ^1H NMR and the ^{13}C NMR spectra was a clear indication of analogous dimetallic structures. Furthermore, we were fortunate to obtain single crystals of both complexes and their single-crystal X-ray analyses confirmed that they displayed similar structures as represented in Figure 6 and Figure 7. The selected bond lengths and angles for **8** and **9** are provided in Table 4 and Table 5, respectively. Complexes **7**–**9** displayed parallel structural features with small differences in bond lengths and bond angles.

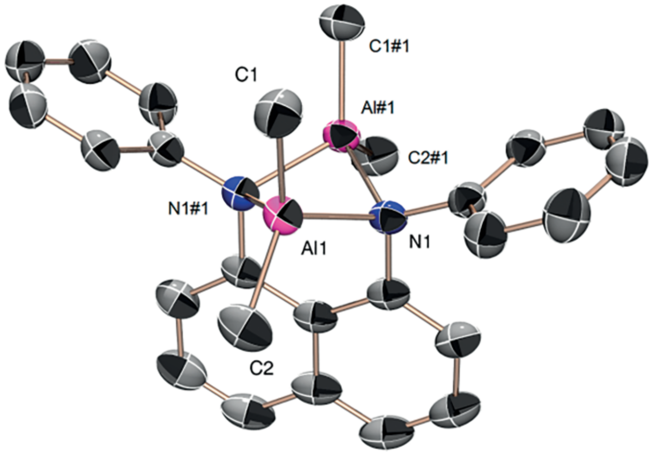

Figure 6. The molecular structure for $(AlMe_2)_2[1,8\text{-}(PhN)_2C_{10}H_6]$ (**8**). Hydrogen atoms have been omitted for clarity. The thermal ellipsoids are shown at 50 % probability level.

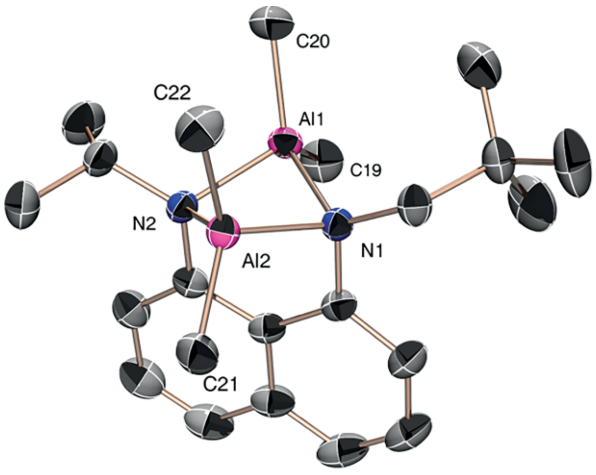

Figure 7. The molecular structure for $(AlMe_2)_2[1,8\text{-}(iPrN)(NpN)C_{10}H_6]$ (**9**). Hydrogen atoms have been omitted for clarity. The thermal ellipsoids are shown at 50 % probability level.

Table 4. Selected bond lengths [Å] and angles [°] for $[Al(CH_3)_2]_2[(PhN)_2C_{10}H_6]$ (**8**).

C(1)–Al(1)	1.9544(16)	C(9)–N(1)	1.4633(16)
C(2)–Al(1)	1.9542(16)	N(1)–Al(1)	1.9868(12)
C(3)–N(1)	1.4491(17)	N(1)–Al(1)#1	1.9966(12)
C(2)–Al(1)–C(1)	118.16(8)	C(3)–N(1)–Al(1)	116.05(8)
C(2)–Al(1)–N(1)	115.05(7)	C(9)–N(1)–Al(1)	108.07(8)
C(1)–Al(1)–N(1)	111.38(6)	C(3)–N(1)–Al(1)#1	119.73(8)
C(2)–Al(1)–N(1)#1	112.44(6)	C(9)–N(1)–Al(1)#1	105.24(8)
C(1)–Al(1)–N(1)#1	114.29(6)		
N(1)–Al(1)–N(1)#1	79.43(6)		

Table 5. Selected bond lengths [Å] and angles [°] for $[Al(CH_3)_2]_2[(iPrN)(NpN)C_{10}H_6]$ (**9**).

C(19)–Al(1)	1.9544(17)	Al(1)–N(2)	1.9832(13)
C(20)–Al(1)	1.9680(17)	Al(1)–N(1)	1.9909(12)
C(21)–Al(2)	1.9570(16)	Al(2)–N(2)	1.9734(12)
C(22)–Al(2)	1.9603(16)	Al(2)–N(1)	1.9961(12)
C(19)–Al(1)–C(20)	115.04(8)	C(21)–Al(2)–C(22)	115.81(8)
C(19)–Al(1)–N(2)	114.15(7)	C(21)–Al(2)–N(2)	116.84(7)
C(20)–Al(1)–N(2)	109.85(7)	C(22)–Al(2)–N(2)	111.79(6)
C(19)–Al(1)–N(1)	113.16(7)	C(21)–Al(2)–N(1)	113.04(6)
C(20)–Al(1)–N(1)	118.84(7)	C(22)–Al(2)–N(1)	113.41(7)
N(2)–Al(1)–N(1)	81.17(5)	N(2)–Al(2)–N(1)	81.29(5)
C(1)–N(1)–C(11)	116.27(11)	C(9)–N(2)–C(16)	119.99(11)
C(1)–N(1)–Al(1)	106.65(8)	C(9)–N(2)–Al(2)	107.05(9)
C(11)–N(1)–Al(1)	125.22(9)	C(16)–N(2)–Al(2)	113.44(9)
C(1)–N(1)–Al(2)	102.11(8)	C(9)–N(2)–Al(1)	105.28(9)
C(11)–N(1)–Al(2)	111.32(8)	C(16)–N(2)–Al(1)	116.08(9)
Al(1)–N(1)–Al(2)	89.97(5)	Al(2)–N(2)–Al(1)	90.86(5)

Conclusions

Elimination of hydrogen or methane from borane or trimethylaluminum when reacted with *N*,*N′*-disubstituted-1,8-diaminonaphthalene has been documented as a versatile route to dialkyl- and diaryl-1,8-diamidonaphthalene complexes for group 13. This ligand array supports unexpectedly air-stable, trigonal planar borane compounds $HB[1,8\text{-}(NR)C_{10}H_6]$ (R = *i*Pr, **4** and R = Ph, **5**). Structural analysis combined with computations point to significant B–N $p\pi$–$p\pi$ bonding, a feature that we attribute to the observed stability.

In the case of the trimethylaluminum reactions, the identity of the products as mono- or bimetallic systems supported by the 1,8-diamidonaphthalene dianion depended on stoichiometry as well as substituent identity. The different coordination environments and ligand bonding features were documented by single-crystal X-ray diffraction analyses and the unanticipated bimetallic complexes feature four-membered M_2N_2 rings with puckered butterfly structures. The structural data suggested that the dialkyl and diaryl are stronger σ-bonding ligands compared to trimethylsilyl analogues.

Compounds **4**–**9** represent interesting species as well as building blocks for further group 13 chemistry. Our continuing investigations are focused on variation of the ligand as well as exploring changes to the bonding environment of the group 13 element.

Experimental Section

General: All manipulations were carried out in either a nitrogen filled dry box or under nitrogen using standard Schlenk techniques. Reaction solvent (anhydrous diethyl ether) was sparged with nitrogen then dried by passage through column of activated alumina using an apparatus purchased from Anhydrous Engineering. Deuterated benzene was purchased from Aldrich Chemical Company and was dried by vacuum transfer from potassium. $BH_3{\cdot}SMe_2$, and $AlMe_3$, anhydrous toluene, and anhydrous hexane were purchased from Aldrich Chemical Company and used without further purification. ^1H, ^{13}C, and ^{11}B NMR spectra were run on either a Bruker 300 MHz or Bruker 600 MHz spectrometer using the residual protons of the deuterated solvent for reference. Elemental analyses were performed by G.G. Hatch Stable Isotope Laboratory at the University of Ottawa or Midwest Micro Lab in Indianapolis, IN, USA.

Structural Determinations: The crystals were mounted on thin glass fibers using paraffin oil. Prior to data collection, crystals were cooled to 200 ± 2 K. Data were collected on a Bruker AXS single-crystal diffractometer equipped with a sealed Mo tube source (wavelength 0.71073 Å) and APEX II CCD detector. Raw data collection and processing were performed with Bruker APEX II software package.[21] Semi-empirical absorption corrections based on equivalent reflections were applied.[22] Systematic absences in the diffraction dataset and unit cell parameters were consistent with triclinic $P\bar{1}$ (#2) for **7** and **9**, monoclinic $P2_1/n$ (#14) for **6** and **3**, and $P2_1/c$ (#14) for **5**, monoclinic $C2/c$ (#15) for **8**, orthorhombic $P2_12_12_1$ (#19) for **4**. The structures were solved by direct methods and refined with full-matrix least-squares procedures based on F^2, using SHELXL[23] and WinGX.[24] All non-hydrogen atoms were refined anisotropically. The hydrogen atoms were placed in idealized positions, except for H(1) in **4**, H(1) in **5**, and H(1A), H(2A) in **3** that were located in the difference Fourier map and refined freely. In **4** one of the isopropyl groups is disordered over two positions with 0.61(3):0.39(3) occupancy ratio. It was refined using enhanced rigid-body restraints (RIGU) and constraints (EADP) applied to the atomic displacement parameters. No additional restraints or constraints were used for refinement of **3**, and **5**–**9**.

Preparation of HB[1,8-(N*i*Pr)$_2$C$_{10}$H$_6$] (4): The diamine $(i\text{PrNH})_2C_{10}H_6$ **1** (0.40 g, 1.65 mmol) was dissolved in approximately 30 mL of toluene and transferred to a Schlenk vessel equipped with a Teflon screw cap. To this solution was added $BH_3{\cdot}SMe_2$ (0.140 g, 1.84 mmol) pre-dissolved in toluene. The solution was heated to 60 °C overnight. The volatiles were removed under vacuum and the crude product was crystallized by dissolving in hexane and cooling to –25 °C. The product was isolated as colorless crystals and dried under vacuum (0.397 g, 1.57 mmol, 95 %). ^1H NMR (C_6D_6, 300 MHz): with ^{11}B decoupling δ = 7.20–7.22 (m, 4 H, CH), 6.36–6.41 (m, 2 H, CH), 4.74 (s br, 1 H, BH), 3.67 (sep, 2 H, *J* = 6.03 Hz, $CHMe_2$), 1.12 (d, 12 H, *J* = 6.54, CH_3). ^{13}C NMR (C_6D_6, 300 MHz): δ = 141.85, 137.28, 127.70, 127.10, 118.20, 102.97(C aromatic), 46.69 ($CHMe_2$), 22.86 (CH_3). ^{11}B NMR (C_6D_6, 300 MHz): with ^1H decoupling δ = 25.9 (s BN_2H).

Preparation of HB[1,8-(NC$_6$H$_5$)$_2$C$_{10}$H$_6$] (5): The diamine $(C_6H_5NH)_2C_{10}H_6$ **2** (0.320 g, 1.03 mmol) was dissolved in approximately 30 mL of toluene and transferred to a Schlenk vessel equipped with a Teflon screw cap. To this solution was added $BH_3{\cdot}SMe_2$ (0.14 mL, 1.115 mmol) pre-dissolved in toluene. The solution was heated to 60 °C overnight. The volatiles were removed under vacuum and the crude product was crystallized by dissolving in ether and cooling to –25 °C. The product was isolated as light orange color crystals and dried under vacuum (0.303 g, 0.95 mmol, 92 %). ^1H NMR ($CDCl_3$, 300 MHz): δ = 7.44–7.50 (m, 4 H, CH), 7.30–7.37 (m, 6 H, CH), 7.03–7.14 (m, 4 H, CH), 6.15 (dd, 2 H, CH), 4.26 (s br, 1 H, BH). ^{13}C NMR ($CDCl_3$, 300 MHz): δ = 143.88, 142.97, 136.32, 129.90, 128.25, 127.06, 126.78, 120.32, 118.90, 106.15 (C aromatic). ^{11}B NMR ($CDCl_3$, 300 MHz): with ^1H decoupling δ = 28.4 (s, BN_2H).

Preparation of [μ-1,8-C$_{10}$H$_6$(NC$_6$H$_5$)$_2$](AlMe)(OEt$_2$) (6): The diamine $(C_6H_5NH)_2C_{10}H_6$ **2** (0.310 g, 1.0 mmol) was dissolved in approximately 15 mL of diethyl ether in a round-bottomed flask equipped with a stir bar. To the solution was added a 2.0 M hexanes solution of AlMe3 (0.5 mL, 1.0 mmol). The solution was stirred overnight and turned green, reddish brown, and finally red in color. The volatiles were removed and the product was recrystallized from ether at –25 °C, giving red crystals (0.314 g, 0.74 mmol, 0.74 %). ^1H NMR ($CDCl_3$, 300 MHz): δ = 7.37 (dd, 2 H, CH, *J* = 8.16, 1.32 Hz), 7.13–7.11 (m, 2 H, CH), 6.93–7.07 (m, 6 H, CH), 6.67–6.73 (m, 6 H, CH), 0.24(s, 3 H, CH_3Al). ^{13}C NMR ($CDCl_3$, 300 MHz): δ = 144.93, 140.06, 137.45, 129.09, 126.01, 123.30, 121.10, 118.09, 116.92 (C aromatic), 1.39(CH_3Al).

Preparation of [μ-1,8-C$_{10}$H$_6$(N*i*Pr)$_2$](AlMe$_2$)$_2$ (7): The diamine $(i\text{PrNH})_2C_{10}H_6$ **1** (0.242 g, 1.0 mmol) was dissolved in approximately 15 mL of hexane in a round-bottomed flask equipped with a stir bar. To the solution was added a 2.0 M hexanes solution of AlMe3 (1.0 mL, 2.0 mmol). The solution was stirred overnight as it turned black, then brown. The volatiles were removed to yield a beige solid. The product was recrystallized from ether at –25 °C, affording colorless crystals (0.0174 g, 49 %). ^1H NMR (C_7D_8, 300 MHz): δ = 7.31–6.68 (m, 6 H), 4.03 (sept, 2 H, *J* = 7.14 Hz), 3.58 (m, 1 H), 1.38 (d, 6 H, *J* = 7.05 Hz), 1.28 (d, 6 H, *J* = 6.33 Hz), –0.10 (s, 6 H), –1.18 (s, 6 H). ^{13}C NMR (C_6D_6, 300 MHz): δ = 125.31, 123.25, 122.16, 119.74, 113.44, 111.66(C aromatic), 47.41($CHMe_2$), 47.13($CHMe_2$), 22.49(CH_3), 19.08(CH_3), –5.23($AlMe_2$), –10.95($AlMe_2$).

Preparation of [μ-1,8-C$_{10}$H$_6$(NC$_6$H$_5$)$_2$](AlMe$_2$)$_2$ (8): The diamine $(C_6H_5NH)_2C_{10}H_6$ **2** (0.105 g, 0.5 mmol) was dissolved in approximately 15 mL of diethyl ether in a round-bottomed flask equipped with a stir bar. To this solution was added a 2.0 M hexanes solution of AlMe3 (0.5 mL, 1.0 mmol). The solution was stirred overnight and turned green, then red color. The volatiles were removed and the product was recrystallized from ether at –25 °C, providing red crystals (0.135 g, 0.32 mmol, 65 %). ^1H NMR (C_6D_6, 600 MHz): δ = 7.18–7.28 (m, 9 H), 7.11–7.13 (m, 2 H), 6.93 (t, 3 H, *J* = 7.89 Hz), 6.36(dd, *J* = 7.72, 1.00 Hz, 2 HHz), –0.37 (s, 6 H, $AlMe_2$), –0.64 (s, 6 H, $AlMe_2$).

^{13}C NMR (C_6D_6, 600 MHz): δ = 152.14, 144.11, 135.85, 130.99, 130.03, 126.96, 126.76, 123.39, 121.82, 118.04, 113.85 (C aromatic), –8.15 (CH_3Al), –10.04 (CH_3Al).

Preparation of [μ-1,8-$C_{10}H_6$(N*i*Pr)(NNp)]($AlMe_2$)$_2$ (9): The diamine (*i*PrNH)(NpNH)$C_{10}H_6$ **3** (0.300 g, 1.15 mmol) was dissolved in approximately 15 mL of diethyl ether in a round-bottomed flask equipped with a stir bar. To this solution was added a 2.0 M hexanes solution of $AlMe_3$ (1.15 mL, 2.30 mmol). resulting in a green solution. The solution was stirred overnight and turned to a pinkish red color. The volatiles were removed and the product was recrystallized from ether at –25 °C, providing red crystals (0.25 g, 0.66 mmol, 57 %). ^{1}H NMR (C_6D_6, 300 MHz): δ = 7.22–6.89 (m, 6 H), 4.02 (sept, 1 H, *J* = 7.11 Hz), 3.29(s, 2 H), 1.28 (d, 6 H, *J* = 7.20 Hz), 0.95 (2, 9 H), –0.18 (s, 6 H), –1.09 (s, 6 H). ^{13}C{H} NMR (C_6D_6, 300 MHz): δ = 147.79, 144.23, 136.02, 125.26, 125.16, 123.72, 123.19, 122.185, 113.63, 112.76 (C aromatic), 56.90(CH_2Me_3), 47.55($CHMe_2$), 30.75(CMe_3), 18.99(CH_3), 0.99(CH_3), –7.70($AlMe_2$), –10.66($AlMe_2$)

Acknowledgments

We thank the Natural Sciences and Engineering Research Council (NSERC) of Canada, the Saudi Arabian Cultural Bureau, and the Canada Research Chairs Program for funding as well as Canada Foundation for Innovation for computing resources.

Keywords: Aluminum · Diaminonaphthalene · Boranes · Hydrides · Organometallic chemistry

[1] C. Camp, J. Arnold, *Dalton Trans.* **2016**, *45*, 14462–14498.
[2] Y. C. Tsai, *Coord. Chem. Rev.* **2012**, *256*, 722–758.
[3] M. Asay, C. Jones, M. Driess, *Chem. Rev.* **2011**, *111*, 354–396.
[4] L. Bourget-Merle, M. F. Lappert, J. R. Severn, *Chem. Rev.* **2002**, *102*, 3031–3065.
[5] Z. Yang, X. Ma, H. W. Roesky, Y. Yang, V. M. Jiménez-Pérez, J. Magull, A. Ringe, P. G. Jones, *Eur. J. Inorg. Chem.* **2007**, 4919–4922.
[6] V. M. Jimenez-Perez, B. M. Munoz-Flores, H. W. Roesky, T. Schulz, A. Pal, T. Beck, Z. Yang, D. Stalke, R. Santillan, M. Witt, *Eur. J. Inorg. Chem.* **2008**, 2238–2243.
[7] T. Riehm, H. Wadepohl, L. H. Gade, *Inorg. Chem.* **2008**, *47*, 11467–11469.
[8] S. C. Martens, T. Riehm, H. Wadepohl, L. H. Gade, *Eur. J. Inorg. Chem.* **2012**, 3039–3046.
[9] C. H. Lee, Y.-H. La, S. J. Park, J. W. Park, *Organometallics* **1998**, *17*, 3648–3655.
[10] P. Bazinet, G. P. A. Yap, G. A. DiLabio, D. S. Richeson, *Inorg. Chem.* **2005**, *44*, 4616–4621.
[11] G. Rimmler, C. Krieger, F. A. Neugebauer, *Chem. Ber.* **1992**, *125*, 723–728.
[12] N. Lavoie, S. I. Gorelsky, Z. Liu, T. J. Burchell, G. P. A. Yap, D. S. Richeson, *Inorg. Chem.* **2010**, *49*, 5231–5240.
[13] H. A. Spinney, I. Korobkov, G. A. DiLabio, G. P. A. Yap, D. S. Richeson, *Organometallics* **2007**, *26*, 4972–4982.
[14] P. Bazinet, G. P. A. Yap, D. S. Richeson, *J. Am. Chem. Soc.* **2001**, *123*, 11162–11167.
[15] P. Bazinet, T. G. Ong, J. S. O'Brien, N. Lavoie, E. Bell, G. P. A. Yap, I. Korobkov, D. S. Richeson, *Organometallics* **2007**, *26*, 2885–2895.
[16] H. A. Spinney, I. Korobkov, D. S. Richeson, *Chem. Commun.* **2007**, 1647–1649.
[17] H. A. Spinney, G. P. A. Yap, I. Korobkov, G. DiLabio, D. S. Richeson, *Organometallics* **2006**, *25*, 3541–3543.
[18] L. Weber, E. Dobbert, H. Stammler, B. Neumann, R. Boese, D. Bläser, *Eur. J. Inorg. Chem.* **1999**, 491–497.
[19] D. T. Carey, F. S. Mair, R. G. Pritchard, J. E. Warren, R. J. Woods, *Dalton Trans.* **2003**, 3792–3798.
[20] M. J. Frisch, G. W. Trucks, H. B. Schlegel, G. E. Scuseria, M. A. Robb, J. R. Cheeseman, G. Scalmani, V. Barone, B. Mennucci, G. A. Petersson, H. Nakatsuji, M. Caricato, X. Li, H. P. Hratchian, A. F. Izmaylov, J. Bloino, G. Zheng, J. L. Sonnenberg, M. Hada, M. Ehara, K. Toyota, R. Fukuda, J. Hasegawa, M. Ishida, T. Nakajima, Y. Honda, O. Kitao, H. Nakai, T. Vreven, J. A. Montgomery Jr., J. E. Peralta, F. Ogliaro, M. Bearpark, J. J. Heyd, E. Brothers, K. N. Kudin, V. N. Staroverov, R. Kobayashi, J. Normand, K. Raghavachari, A. Rendell, J. C. Burant, S. S. Iyengar, J. Tomasi, M. Cossi, N. Rega, J. M. Millam, M. Klene, J. E. Knox, J. B. Cross, V. Bakken, C. Adamo, J. Jaramillo, R. Gomperts, R. E. Stratmann, O. Yazyev, A. J. Austin, R. Cammi, C. Pomelli, J. W. Ochterski, R. L. Martin, K. Morokuma, V. G. Zakrzewski, G. A. Voth, P. Salvador, J. J. Dannenberg, S. Dapprich, A. D. Daniels, Ö. Farkas, J. B. Foresman, J. V. Ortiz, J. Cioslowski, D. J. Fox, *Gaussian 09, Revision A.02*, Gaussian, Inc., Wallingford CT, **2016**.
[21] APEX2 Software Suite v **2012**. Bruker AXS Inc., Madison, Wisconsin, **2012**.
[22] SADABS Bruker AXS Inc. Madison Wisconsin USA, **2014**.
[23] G. M. Sheldrick, *Acta Crystallogr., Sect. C Struct. Chem.* **2015**, *71*, 3–8.
[24] L. J. Farrugia, *J. Appl. Crystallogr.* **1999**, *32*, 837–838.

Received: March 6, 2018

Organometallic Chemistry

*S. Lee, N. Almalki, B. Gabidullin, D. Richeson** 1–8

***N,N′*-Diamidonaphthalene as a Versatile Ligand to Stabilize Mono- and Bimetallic Complexes of Group 13**

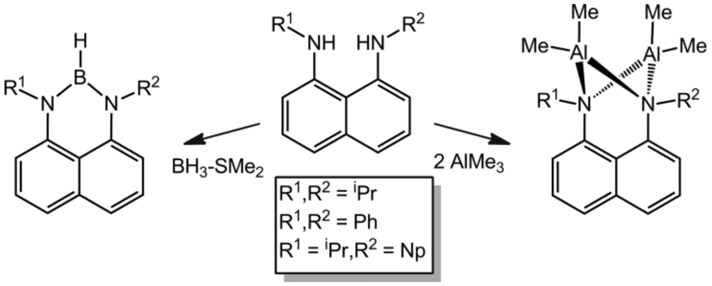

Borohydride and alkylaluminum species are supported by disubstituted 1,8-diamidonaphthalene ligation.

---

https://doi.org/10.1002/ejic.201800297